Plan-View and Cross-Sectional Photoluminescence Imaging Analyses of Threading Dislocations in 4H-SiC Epilayers

Japanese Journal of Applied Physics **52** (2013) 04CP09 **REGULAR PAPER**
http://dx.doi.org/**10.7567/JJAP.52.04CP09**

Plan-View and Cross-Sectional Photoluminescence Imaging Analyses of Threading Dislocations in 4H-SiC Epilayers

Masahiro Nagano, Isaho Kamata, and Hidekazu Tsuchida

Central Research Institute of Electric Power Industry (CRIEPI), Yokosuka, Kanagawa 240-0196, Japan

Received September 23, 2012; accepted January 5, 2013; published online April 22, 2013

We performed a plan-view and cross-sectional photoluminescence (PL) imaging and a spectral analysis of threading dislocations in 4H-SiC epilayers in the near-infrared region. The bright PL spots of threading screw dislocations (TSDs) and threading edge dislocations (TEDs) observed in the plan-view PL imaging are compared with the grazing incidence synchrotron X-ray topography contrast, and precise discrimination of threading dislocations using the PL technique and the direct acquisition of Burgers vector directions of TEDs are demonstrated. The inclination angles of TSDs and TEDs across a thick epilayer are revealed by the cross-sectional PL imaging, and the variations in the plan-view PL appearances of the threading dislocations are confirmed to originate from the line directions of such dislocations.

1. Introduction

Silicon carbide (SiC) is a desirable semiconductor material for high-power and high-temperature applications owing to its wide bandgap and large critical breakdown field. However, a high density of dislocations, including basal plane dislocations (BPDs), threading screw dislocations (TSDs) and threading edge dislocations (TEDs), still exist in substrates and epilayers, which can impair the power device performance. Typical densities of TSDs and TEDs are 10^2–10^3 and 10^3–$10^4\,\mathrm{cm}^{-2}$, respectively in 4H-SiC substrates and epilayers, while those of BPDs are 10^2–$10^4\,\mathrm{cm}^{-2}$ in substrates and 10–$10^2\,\mathrm{cm}^{-2}$ in epilayers, respectively.

Photoluminescence (PL) imaging is a non-destructive technique with a high spatial resolution for detecting dislocations in semiconductor materials. Grazing incidence synchrotron X-ray topography is also a powerful and non-destructive tool for determining the spatial locations of dislocations and their Burgers vector in 4H-SiC, although it requires a special facility. PL techniques, conversely, can be performed in individual laboratories or factories, making it possible to apply them as in-line analysis. Tajima et al. firstly demonstrated the PL mapping of a 1.3 eV (~950 nm) band for an entire 6H-SiC wafer showing dark PL spots and lines that correspond to micropipes and dislocations forming small-angle grain boundaries.[1)] Stahlbush et al. conducted PL imaging in the near-IR region (800–1000 nm) for 4H-SiC epilayers and obtained bright PL spots and lines corresponding to threading dislocations and BPDs, respectively.[2)] Their group also succeeded in the acquisition of the PL spectra of BPDs, TSDs, and TEDs in 4H-SiC epilayers and the one-to-one correspondence between bright PL spots of TSDs and TEDs and their KOH pit patterns.[3,4)] Feng et al. also showed PL contrast in the near-band-edge region (390 nm) for BPDs, TSDs and TEDs in 4H-SiC epilayers as dark PL lines or spots.[5)]

In previous studies of PL imaging of dislocations in 4H- and 6H-SiC, the spatial distributions of TSDs and TEDs were monitored, although information on the Burgers vector directions and inclination angles of dislocations could not be obtained. The distributions of Burgers vector directions[6)] and line directions of threading dislocations across a wafer can lead to better understanding of the SiC bulk and epitaxial growth processes as well as of the effect of each dislocation on the electrical performance of SiC devices. In this study, we performed a plan-view and cross-sectional PL imaging and a spectral analysis of threading dislocations in 4H-SiC epilayers in the near-IR region and demonstrate the precise discrimination of threading dislocations using the PL technique for obtaining information on the Burgers vector directions of TEDs and the inclination angles of TSDs and TEDs across a thick epilayer.

2. Experimental Procedure

Nitrogen-doped n-type thick (140–250 μm) 4H-SiC epilayers with a low doping concentration ($N_\mathrm{d} - N_\mathrm{a}$) of $10^{14}\,\mathrm{cm}^{-3}$ were used as the specimens in this study. The epilayers were grown on Si-face 4H-SiC n-type conductive substrates with an off-cut angle of 8° towards $[11\bar{2}0]$ in a vertical hot-wall reactor.[7)]

The PL images were detected using a cooled CCD camera attached to an optical microscope at room temperature. The 363.8 nm line of a cw Ar laser was used as the excitation light. The laser is operated at 100 mW at an incident beam angle of 30° normal to the sample surface. The beam area is ~1 cm^2 with an oval shape at the sample surface. The spatial resolution is ~0.7 μm in the experiments. The PL spectrum analysis of the dislocations was performed using optical bandpass filters with an FWHM of ±5–7 nm attached to the microscope at room temperature and 78 K. In the observation at 78 K, the samples were placed under vacuum, and the sample stage was cooled using liquid nitrogen. To distinguish TSDs and TEDs and their Burgers vector directions, grazing incidence synchrotron X-ray topography was performed with $\boldsymbol{g} = 11\bar{2}8$ and $\lambda = 1.541$ Å at SPring-8. Molten KOH etching at 480 °C for 1–3 min was employed to determine the spatial locations of the threading dislocations on the (0001) sample surface.

3. Results and Discussion

We firstly evaluated the region that can to be imaged from the surface by the PL technique using a very thick (~250 μm) layer. Figure 1 shows a plan-view PL image taken with a high-pass filter at 700 nm of the epilayer. Bright PL lines in Fig. 1 correspond to BPDs in the epilayer. The length of the BPD luminescence along the step flow direction is ~1600 μm which corresponds to a depth of

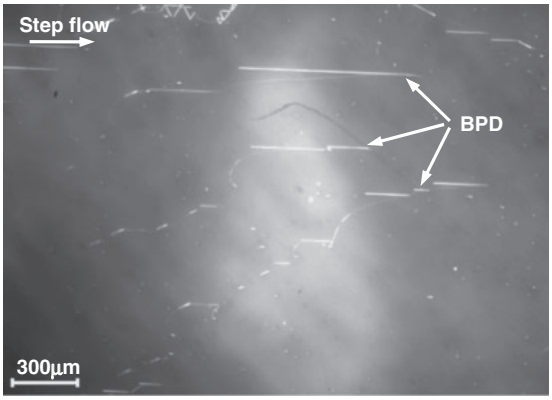

Fig. 1. PL image taken for a very thick epilayer (~250 μm) with a high-pass filter at 700 nm.

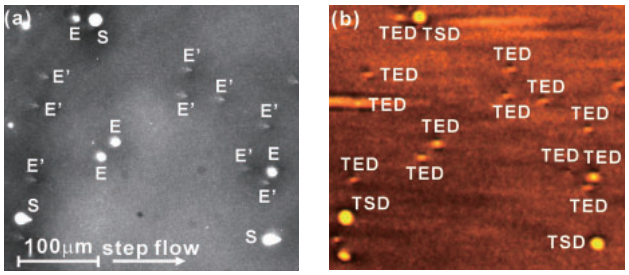

Fig. 2. (Color) (a) Plan-view PL image taken with a bandpass filter at 900 ± 5 nm and (b) grazing incidence synchrotron X-ray topography image ($\boldsymbol{g} = 11\bar{2}8$) for an identical area of a 4H-SiC epilayer.

~220 μm from the surface, while the penetration length of the excitation laser beam ($\lambda = 363.8$ nm) is estimated to be ~120 μm.[8] This indicates that excited carriers diffuse into the deeper region of the epilayer and create PL images of the dislocations even at a depth of ~220 μm from the surface.

Figure 2 shows a plan-view PL image with a bandpass filter at 900 ± 5 nm and a grazing incidence synchrotron X-ray topography image taken for an identical area of a 140-μm-thick 4H-SiC epilayer. In the PL image, we find bright spots with varying appearances. In the X-ray topography image, the TSDs and TEDs exhibit a relatively large circular bright contrast and a short segment of contrast, respectively.[9] In the comparison of the PL and X-ray topography images, one-to-one correlations are confirmed between bright spots in the PL image and the topography defect contrast of TSDs and TEDs.

From the collations with the X-ray topography defect contrast of each threading dislocation, it is confirmed that the TSDs exhibit relatively large PL spots (marked S) compared with TEDs, as indicated in Fig. 2(a). Exceptionally, only minor TSDs showing a small spot are found. Many TSDs exhibit a large-sized circular PL appearance, while some of them accompany a short bright segment extending along the step flow direction or show an appearance slightly extending along the step flow direction [TSD at bottom right in Fig. 2(a)]. The TEDs are confirmed as having two different PL appearances, marked E or E′ in Fig. 2(a). The type-E TEDs exhibit a medium-sized circular PL appearance, while type-E′ TEDs show a small-sized PL appearance

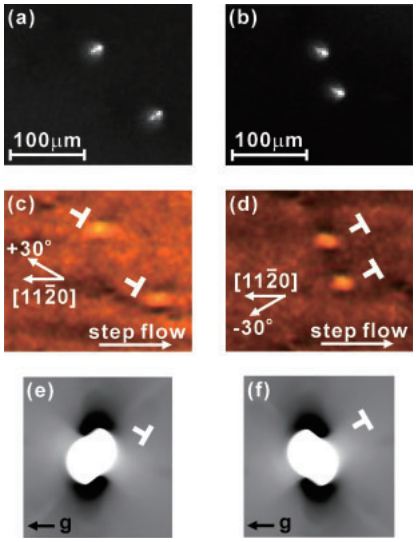

Fig. 3. (Color) Plan-view PL image (900 ± 5 nm) and grazing incidence synchrotron X-ray topography image ($\boldsymbol{g} = 11\bar{2}8$) of TEDs with an extra half plane pointing towards +30° [(a) PL, (c) X-ray topography, (e) ray-tracing simulation[6]] and −30° [(b) PL, (d) X-ray topography, (f) ray-tracing simulation[6]] clockwise from the off-cut [11$\bar{2}$0] direction.

with a short bright segment extending along the step flow direction with a slight tilt angle. No changes in the PL appearances were observed when a different incident direction of the excitation laser was employed, indicating that the unique structure of each threading dislocation determines the PL appearances.

The directions of the Burgers vector of the TSDs and TEDs are analyzed by observing defect contrast appearances in the X-ray topography image.[6] No correlations are found between the PL appearances of the TSDs and their Burgers vector directions (clockwise or counter-clockwise) of the screw component along the *c*-axis. Note that recent studies suggest the existences of mixed-type ($c + a$) threading dislocations in 4H-SiC,[10–12] although both 1*c* and $c + a$ dislocations can be treated as TSDs in our X-ray topography analysis. In addition, TSDs exhibiting a PL appearance accompanying a short bright segment or a segment slightly extending along the step flow direction match the slightly enlarged defect topography contrast along the step flow direction.

Six types of TEDs having a $1/3\langle 11\bar{2}0\rangle$ type Burgers vector with different directions are confirmed in the X-ray topography image.[6] By comparisons between the obtained PL and X-ray topography images of each TED, differences in the PL appearance of TEDs are found to correlate with their Burgers vector directions. TEDs with an extra half-plane pointing towards ±30° from the off-cut [11$\bar{2}$0] direction are confirmed to show the type-E PL appearance, while other types of TEDs show type-E′ PL appearances. The type-E TEDs are further divided into two kinds by detailed appearance. Figures 3(a)–3(d) show two sets of PL and X-ray topography images of the type-E TEDs found in different areas. The contrast of the PL images is adjusted to express more detailed appearances. The TEDs with an extra half plane pointing towards +30° [Figs. 3(a) and 3(c)] and −30° [Figs. 3(b) and 3(d)] clockwise from the off-cut [11$\bar{2}$0]

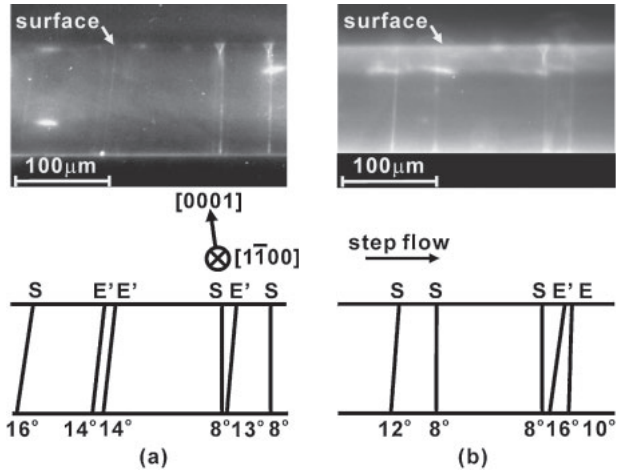

Fig. 4. Cross-sectional PL images (900 ± 5 nm) for two different positions of an 8°-off 4H-SiC epilayer, and schematic drawings of the observed PL lines of TSDs (marked S) and TEDs (marked E or E′) and the inclination angles measured from the *c*-axis.

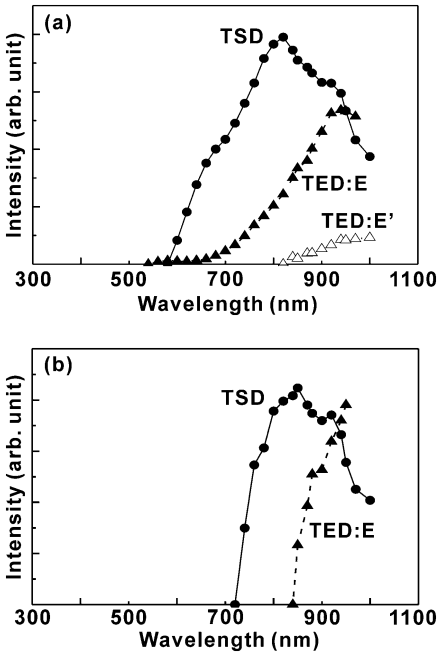

Fig. 5. PL spectra of TSDs and TEDs in 4H-SiC epilayers at (a) RT and (b) 78 K.

direction show a PL bright core (short segment) tilting about -30 and $+30°$ from the [11$\bar{2}$0] direction, respectively. Figures 3(e) and 3(f) show ray-tracing simulation[6] images of the TEDs with an extra half plane pointing towards $+30$ and $-30°$ clockwise from the off-cut [11$\bar{2}$0] direction, respectively. In the comparison between the PL images [Figs. 3(a) and 3(b)] and the ray-tracing images [Figs. 3(e) and 3(f)], the appearances of bright PL spots and ray-tracing simulation images of the type-E TEDs are found to resemble each other. The coincidence of the PL and ray-tracing simulation images indicates that the PL appearances of the type-E TEDs are affected by the strain field around the dislocation core, since the ray-tracing simulation images reflect the patterns of strain fields (elastic displacement function)[13] for the corresponding types of TEDs. This may be the first demonstration of the direct acquisition of the Burgers vector directions of TEDs by PL techniques.

To investigate the dislocation line of threading dislocations, cross-sectional PL imaging was performed on (1$\bar{1}$00) cut sections of an epilayer. Figure 4 shows cross-sectional PL images of a 140-μm-thick epilayer, which were taken using a 900 nm bandpass filter after fine-polishing the (1$\bar{1}$00) observed surface using diamond slurry. The substrate regions are masked in this cross-sectional imaging, since strong infrared luminescence from the substrate reduces the PL image contrast of threading dislocations in the epilayer. Bright PL lines across the epilayer in Fig. 4 correspond to those of threading dislocations, revealing dislocations propagation throughout the epilayer towards the surface from the epilayer/substrate interface. Confirming the precise positions of the dislocation on the (0001) surface by collation with the grazing incidence synchrotron X-ray topography image and KOH etch pit pattern, the PL lines are identified as those of TSDs and TEDs, located within ~180 μm of the (1$\bar{1}$00) observed surface.

The schematic drawings in Fig. 4 summarize the correspondences of the observed PL lines and dislocation types as well as the inclination angles measured from the *c*-axis towards the step flow direction. The TSDs are found to have various inclination angles. The type-E TEDs are confirmed to propagate throughout the epilayer in the direction almost normal to the surface (~8° from the *c*-axis), while the inclination angles of the type-E′ TEDs exceed (>10°) those of the type-E TEDs. Evidence of the large inclination angles of the type-E′ TEDs explains why their plan-view PL appearance shows a short bright segment extending along the step flow direction, while type-E TEDs almost normal to the surface exhibit a circular PL appearance. TSDs with a large inclination angle also match those exhibiting slightly enlarged defect topography contrasts along the step flow direction. This indicates that the plan-view PL appearance accompanying a short bright segment or a segment slightly extending along the step flow direction in Fig. 2(a) correlates with their propagation angle of what across the epilayer.

Figure 5 shows the PL spectra of TSDs and the type-E and type-E′ TEDs at RT and 78 K. The PL from the TSDs is observed within the range of 600–1000 nm, while the peak position varies between 800–950 nm among different TSDs. The origin of the variations in the PL spectra of TSDs is unclear at this time but variations of impurities or defects surrounding the core of TSDs may be considered as the reason. The PL spectra of the TEDs are broad in the range above 700 nm and peak at >900 nm in room-temperature measurements, while the spectra becomes sharp in low-temperature measurements at 78 K. Liu et al. have reported that TSDs and TEDs exhibit spectral peaks at 800–850 and ~600 nm, respectively.[4] Although the PL spectra obtained for TSDs in this study resemble those in the earlier report, the spectral ranges for TEDs differ significantly. The reason for the difference in the TED spectra is not yet clear. However, Liu et al. found that the near-IR band of C-core partial dislocations (PDs) saturates when the electron–hole (e–h) concentration increases.[3] Further study is necessary

to investigate the spectral changes of TEDs with different excitation intensities. No significant spectral difference is found between the type-E and type-E′ TEDs, while the PL intensity of the type-E′ TED is much weaker than that of the type-E TED. The stronger luminescence of the type-E TEDs than of the type-E′ TEDs is explained by their propagation angles across the epilayer. Luminescence from dislocations, even ~220 μm deep from the surface, are detected under the plan-view PL conditions, as confirmed in Fig. 1. Considerable luminescence from shallow to deep regions accumulates in a small area if the dislocations are normal to the surface, while luminescence is distributed linearly if the dislocations have a significant inclined angle.

The luminescence mechanisms of threading dislocations are under discussion, while the core and bandgap structures and the luminescence mechanisms of Si- and C-core PDs, which are formed by the dissociation of a perfect BPD with a $1/3\langle 11\bar{2}0\rangle$ type Burgers vector, have been discussed in the literature.[3,14,15] Chung et al. investigated the electric potential distribution of TSDs and estimated the ionization energy as 0.89 ± 0.22 eV.[16] They also pointed out that a bond reconstruction along threading dislocation cores can lead to the formation of traps similar to those of PDs. Liu et al. reported the PL spectra of Si- and C-core PDs in a 4H-SiC epilayer.[3,4] Note that their PL spectra of Si-core PD (600–900 nm peaking at ~800 nm)[4] and C-core PD (>600 nm peaking at ~900 nm)[3] resemble those of TSDs and TEDs shown in Fig. 5, respectively, quite closely. Although neither the core structures of TSDs and TEDs nor $c + a$ dislocations are determined at this time, similar PL spectra indicate that similar or common mechanisms might be involved in the luminescence of the threading dislocations and Si- or C-core PDs which consist of Si–Si bonds and C–C bonds, respectively.

4. Summary

In summary, one-to-one correlations are confirmed between the plan-view PL appearance and defect contrast in the grazing incidence synchrotron X-ray topography of threading dislocations in 4H-SiC epilayers. The TSDs and TEDs were distinguishable by PL spot size and spectrum, while the TSDs exhibit a larger PL spot with a spectral peak at 800–950 nm and the TEDs show a smaller PL spot at >950 nm. The TEDs with an extra half plane pointing towards ±30° from the off-cut $[11\bar{2}0]$ direction show a medium-sized PL appearance, while the other types of TEDs show a small PL appearance with a short bright segment extending along the step flow direction with a small tilt angle. We have also succeeded in the cross-sectional PL imaging of a thick 4H-SiC epilayer revealing the inclination angles of threading dislocations. TEDs with an extra half plane pointing towards ±30° from the off-cut direction are confirmed to propagate throughout the epilayer in a direction almost normal to the surface, while the inclination angles of the other types of TEDs incline towards the step flow direction. It is also confirmed that the dislocation lines of the TSDs and TEDs across the epilayer affect plan-view PL appearances, where the appearance accompanying a short bright segment or slightly extending along the step flow direction correlates with their propagation angle of what across the epilayer.

Acknowledgements

This research is partly supported by the Japan Society for the Promotion of Science (JSPS) through its "Funding Program for World-Leading Innovative R&D on Science and Technology (FIRST Program)".

1) M. Tajima, E. Higashi, T. Hayashi, H. Kinoshita, and H. Shiomi: Appl. Phys. Lett. **86** (2005) 061914.
2) R. E. Stahlbush, K. X. Liu, Q. Zhang, and J. J. Sumakeris: Mater. Sci. Forum **556–557** (2007) 295.
3) K. X. Liu, R. E. Stahlbush, S. I. Maximenko, and J. D. Caldwell: Appl. Phys. Lett. **90** (2007) 153503.
4) K. X. Liu, X. Zhang, R. E. Stahlbush, M. Skowronski, and J. D. Caldwell: Mater. Sci. Forum **600–603** (2009) 345.
5) G. Feng, J. Suda, and T. Kimoto: Jpn. J. Appl. Phys. **49** (2010) 090201.
6) I. Kamata, M. Nagano, H. Tsuchida, Yi. Chen, and M. Dudley: J. Cryst. Growth **311** (2009) 1416.
7) M. Ito, L. Storasta, and H. Tsuchida: Appl. Phys. Express **1** (2008) 015001.
8) S. G. Sridhara, T. J. Eperjesi, R. P. Devaty, and W. J. Choyke: Mater. Sci. Eng. B **61–62** (1999) 229.
9) H. Tsuchida, I. Kamata, M. Nagano, L. Storasta, and T. Miyanagi: Mater. Sci. Forum **556–557** (2007) 271.
10) F. Wu, H. Wang, S. Byrappa, B. Raghothamachar, M. Dudley, E. K. Sanchez, D. Hansen, R. Drachev, S. G. Mueller, and M. J. Loboda: Mater. Sci. Forum **717–720** (2012) 343.
11) S. Hamada, H. Yoshioka, H. Kawami, N. Nakamura, Y. Setoguchi, T. Matsunami, K. Nishikawa, and T. Isshiki: Mater. Sci. Forum **725** (2012) 31.
12) Y. Sugawara, M. Nakamori, Y.-Z. Yao, Y. Ishikawa, K. Danno, H. Suzuki, T. Bessho, S. Yamaguchi, K. Nishikawa, and Y. Ikuhara: Appl. Phys. Express **5** (2012) 081301.
13) W. M. Vetter and M. Dudley: J. Appl. Crystallogr. **37** (2004) 200.
14) A. T. Blumenau, C. J. Fall, R. Jones, S. Öberg, T. Frauenheim, and P. R. Briddon: Phys. Rev. B **68** (2003) 174108.
15) G. Savini, M. I. Heggie, and S. Öberg: Faraday Discuss. **134** (2007) 353.
16) S. Chung, R. A. Berechman, M. R. McCartney, and M. Skowronski: J. Appl. Phys. **109** (2011) 034906.